

# Analysis of effect of voltage on surface texture in electrochemical grinding by autocorrelation function

Suvadeep Roy<sup>a,\*</sup>, Ardhendu Bhattacharyya<sup>b</sup>, Simul Banerjee<sup>b</sup>

<sup>a</sup>Variable Energy Cyclotron Center, 1/AF Salt Lake, Kolkata 700064, India

<sup>b</sup>Department of Mechanical Engineering, Jadavpur University, Kolkata 700032, India

Received 26 August 2005; received in revised form 19 March 2007; accepted 28 March 2007

Available online 21 May 2007

## Abstract

The major difficulty faced in electrochemical grinding (ECG) of composite materials is poor surface integrity because of differential dissolution rates of different ingredients present in those materials. In the present investigation an experimental study, organized by statistical procedure, was made to evaluate the effect of the major controllable parameter 'voltage' on the surface finish of P-20 grade cemented carbide. The surface roughness data were analyzed for different voltages. The values of autocorrelation function for different values of lag period were calculated. The periodicity and randomness of surface roughness were identified. They are compared with the similar observations on the conventional diamond grinding of the same material in ECG environment with no application of voltage. A non-dimensional parameter was introduced for that purpose and was termed as 'periodicity to randomness index'. An attempt was made to find out the relative contribution of the electrolytic dissolution under the chosen experimental conditions.

© 2007 Elsevier Ltd. All rights reserved.

**Keywords:** ECG; Autocorrelation function; Electrolytic dissolution; Periodicity to randomness index

## 1. Introduction

Study of machined surface topography evolves with two main objectives: (1) effect of machining parameters like depth of cut, cutting speed, etc. and (2) adverse consequences like fracture, wear, plastic deformation, etc. [1,2]. Functional performance of a surface can be well understood from various features like waviness, roughness which are in turn related to different aspects of the process through which the surface is generated [3]. Therefore, it is essential to study the surface profile to develop a predictive model to evaluate the surface damage. Surface roughness is a non-stationary random data and various statistical parameters have been developed to characterize a machined surface. Vertical or transverse surface roughness parameters like arithmetical mean deviation of profile ( $R_a$ ), 10-point height of macroscopic plainness ( $R_z$ ) or RMS

wavelength of the profile ( $\lambda$ ) do not reveal the actual complexity of the surfaces [4]. However, it is possible by integrated evaluation parameters like autocorrelation function (ACF) ' $C(\tau)$ ', correlation length ' $a$ ' or power spectrum density function ' $P(\omega)$ '. In electrochemical grinding (ECG), removal of material is achieved by combined effect of both mechanical abrasion and electrolytic dissolution [5]. Sintered carbide materials because of their different ingredients are characterized by large-scale heterogeneities in their mechanical and electrochemical properties which are affecting the surface integrity [6]. In the present work ( $\{WC + TiC + TaC/NbC\}$ -Co) cemented carbide of Grade P-20 is chosen as the workpiece material. It is ground by ECG process and also by mechanical grinding process for the purpose of comparison. The mechanical grinding condition in ECG environment is developed by simply switching off the electric power supply, i.e. making applied voltage equal to zero across the electrolytic cell. The relative contribution of mechanical abrasion and electrolytic dissolution is then segregated by analyzing the surface profile using ACF.

\*Corresponding author. Tel.: +91 33 23371230.

E-mail address: [subhodip\\_ray@yahoo.com](mailto:subhodip_ray@yahoo.com) (S. Roy).

## 2. Experiment

Numbers of tiny electrolytic cell are formed during ECG. The workpiece acts as an anode while conducting body of the rotating grinding wheel as the cathode. Anode and cathode are separated by the non-conducting abrasive grits embedded on and projected out of the grinding wheel metal surface. The abrasive grits run in contact with the workpiece surface under a feed force and thus a gap is maintained. Electrolyte is taken into the gap by the pockets formed between the projected grits of the rotating grinding wheel for electrochemical reactions to take place. A nozzle is, therefore, necessary for forcing the electrolyte into the machining zone. A low voltage high current source is applied across the cells in the gap. The voltage ranges from 5 to 30 V. While selection of lower limit of voltage is governed by the onset of electrochemical dissolution (decomposition potential) of the chosen workpiece material, the upper setting of voltage is limited by the occurrence of detrimental sparking phenomena [7].

In the present experimentation, therefore, a metal bonded diamond grinding wheel is selected as cathode tool and is insulated from the rest of the setup. ({WC+TiC+TaC/NbC}-Co) cemented carbide inserts of specification TTW SNUN 190412 equivalent to P-20 grade is chosen as anode workpiece. It is to be mentioned here that cemented carbides though mostly used in machining, yet gaining its importance in alternative applications in mining and drilling in oil and gas installations, metal forming, structural components in construction and as material for tools in the field of forestry engineering [8].

Experimental setup as shown schematically in Fig. 1 was developed in G.C. Sen Memorial Machine Tools Research Laboratory. The major units and corresponding controllable variables are listed below;

- (i) Drive for wheel rotation and its monitoring system to control cutting speed.
- (ii) Job mounting and loading unit together with force monitoring system.
- (iii) Hydraulic system to supply and control the electrolyte flow.
- (iv) Main DC power supply for ECG to control machining voltage.

Several experiments were carried out under different combinations of cutting speed and voltage. The settings of main machining parameters for the present study are summarized in Table 1. During machining of the P-20 grade cemented carbide inserts material is removed mainly by electrolytic dissolution of its ingredients and mechanical abrasion. The surfaces so generated were tested on Talysurf Surface Tester. Each of the surface profiles thus obtained was then scanned and discretized taking sampling interval of the profile as 1  $\mu\text{m}$  and 2000 data in each scan. Fig. 2(a)–(d) shows the measured surface profiles at different voltages at a constant cutting speed 4 m/s. Please

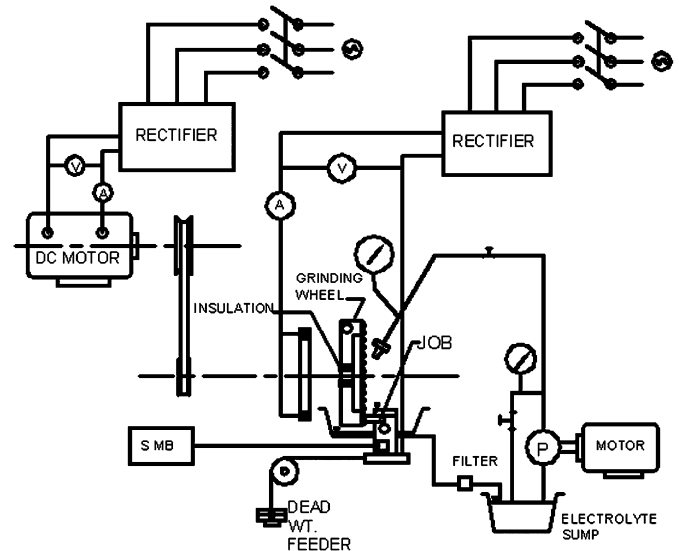


Fig. 1. Schematic of experimental setup.

Table 1  
Major machining parameters

Work piece	Tungsten carbide TTW SNUN 190412
Grinding wheel	Metal bonded diamond wheel with concentration 50
Grain size	80/100 mesh
Grinding speed	4–12 m/s
Voltage	0–15 V
Feed force	2 kg (plunge grinding)
Electrolyte	Sodium nitrate, Concentration 8% by weight
Flow rate	10 l/min

note that the surface profile in Fig. 2(a) with  $V = 0$  V represents results of conventional mechanical grinding in ECG environment without any electrolytic dissolution of workpiece material taking place.

## 3. Analysis

Spatial functions like ACF, structure function or power spectral density function (PSDF) represents all wavelengths, spatial size of features; and autocovariance function (ACVF),  $R(\tau)$ , is the most popular surface texture descriptor, directly interprets how well future values of the function can be predicted based on previous observations. For a function  $y(x)$  two consecutive measurements are taken on the profile data at a distance  $\tau$  (lag) apart and average value of product of such two measurements over the sampling length ' $L$ ' are calculated (Eq. (1)). Plot of these average value vs. different spatial separations  $\tau$ , yields the ACVF curve [4].

$$R(\tau) = \lim_{L \rightarrow \infty} \frac{1}{L} \int_0^L y(x)y(x+\tau) dx. \quad (1)$$

Normalized form of ACVF is called ACF [3] and it is given by [4]

$$C(\tau) = \frac{R(\tau) - m^2}{\sigma^2}, \quad (2)$$

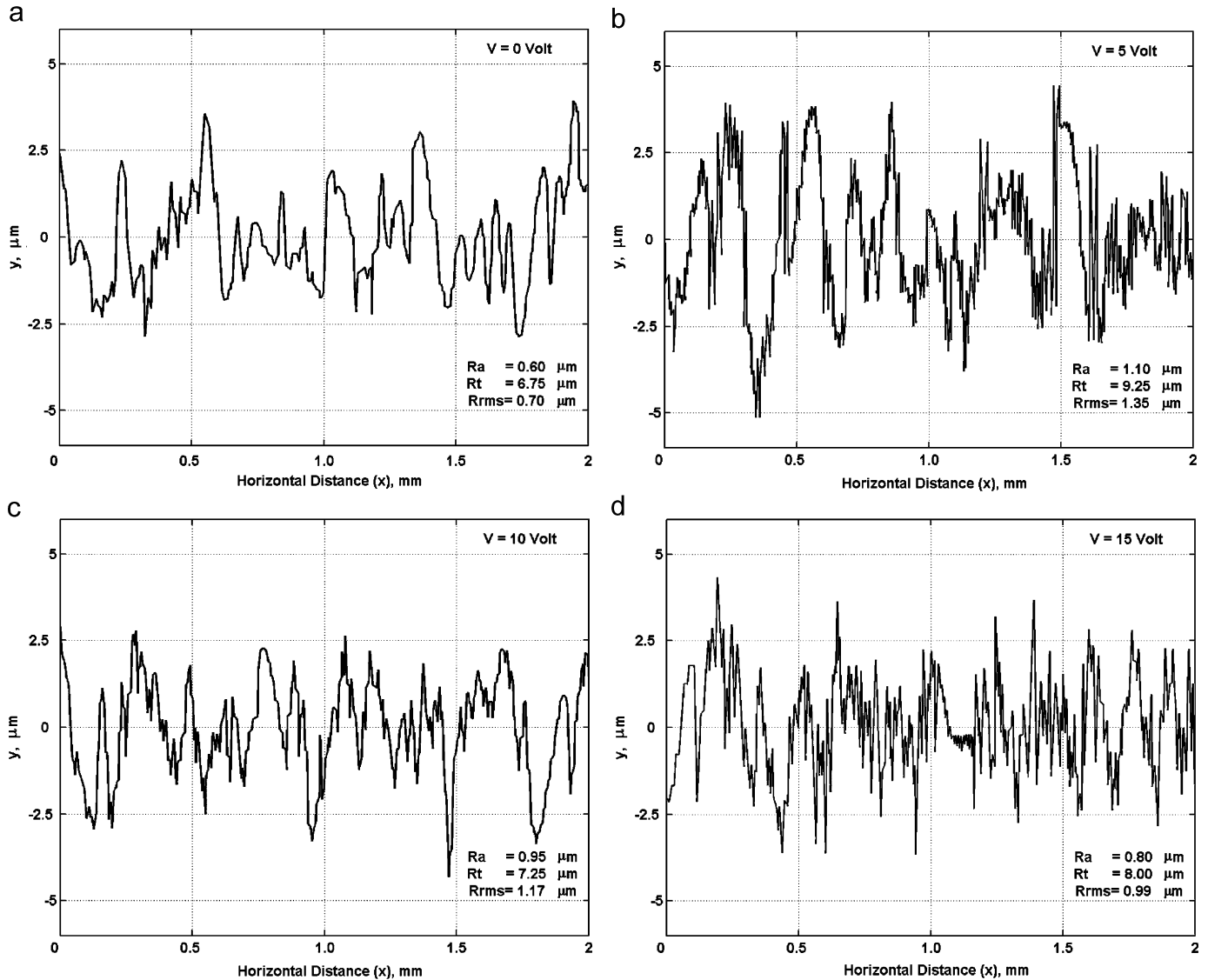


Fig. 2. (a) Surface profile measured by Talysurf for 0 V at cutting speed 4 m/s. (b) Surface profile measured by Talysurf for 5 V at cutting speed 4 m/s. (c) Surface profile measured by Talysurf for 10 V at cutting speed 4 m/s. (d) Surface profile measured by Talysurf for 15 V at cutting speed 4 m/s.

where  $m$  and  $\sigma$  are mean and standard deviation defined by the following equations

$$\sigma^2 = m^2 - R(0) \quad (2a)$$

$$m^2 = R(\infty) \quad (2b)$$

ACF will be maximum and equal to 1 for zero spatial separation and then gradually decays with the increase of  $\tau$ . In case of a surface profile containing wide band randomness, it decays exponentially [9]. On the other hand, for the surface profiles having deterministic periodicities, ACF would attain a peak when lag is a multiple of wavelengths ( $\lambda$ ) signifying that the surface replicates itself at a spatial separation of  $\lambda$  [9]. Between these two extremes, real engineering surfaces are found to be a case of superposition of a periodic function with random distortions (Fig. 3(a)–(d)).

Therefore, we have decomposed the ACF data following a combination of additive and multiplicative model [10] given by

$$C(\tau) = \sum_i A_i \exp(-\tau/\beta_i) \sin(\omega_i\tau + \phi_i), \quad (3)$$

where  $A_i$  are the constants,  $\beta_i$  the decay exponents,  $\omega_i$  the carrier wave frequencies, and  $\phi_i$  the phase differences.

The shorter wavelength components, whose maximum cumulative amplitude is below 5% of the original signal, are filtered out. Out of remaining ACF components, similar frequency signals for different voltage conditions are sorted out (Fig. 4(a)–(e)). The length over which the value of the exponential component of ACF drops down to 10% of its initial value gives an indication about how quickly the random event dies out and it is termed as correlation length ( $\beta_0$ ). Higher value of  $\beta_0$  indicates that the random characteristic continues over a larger length and

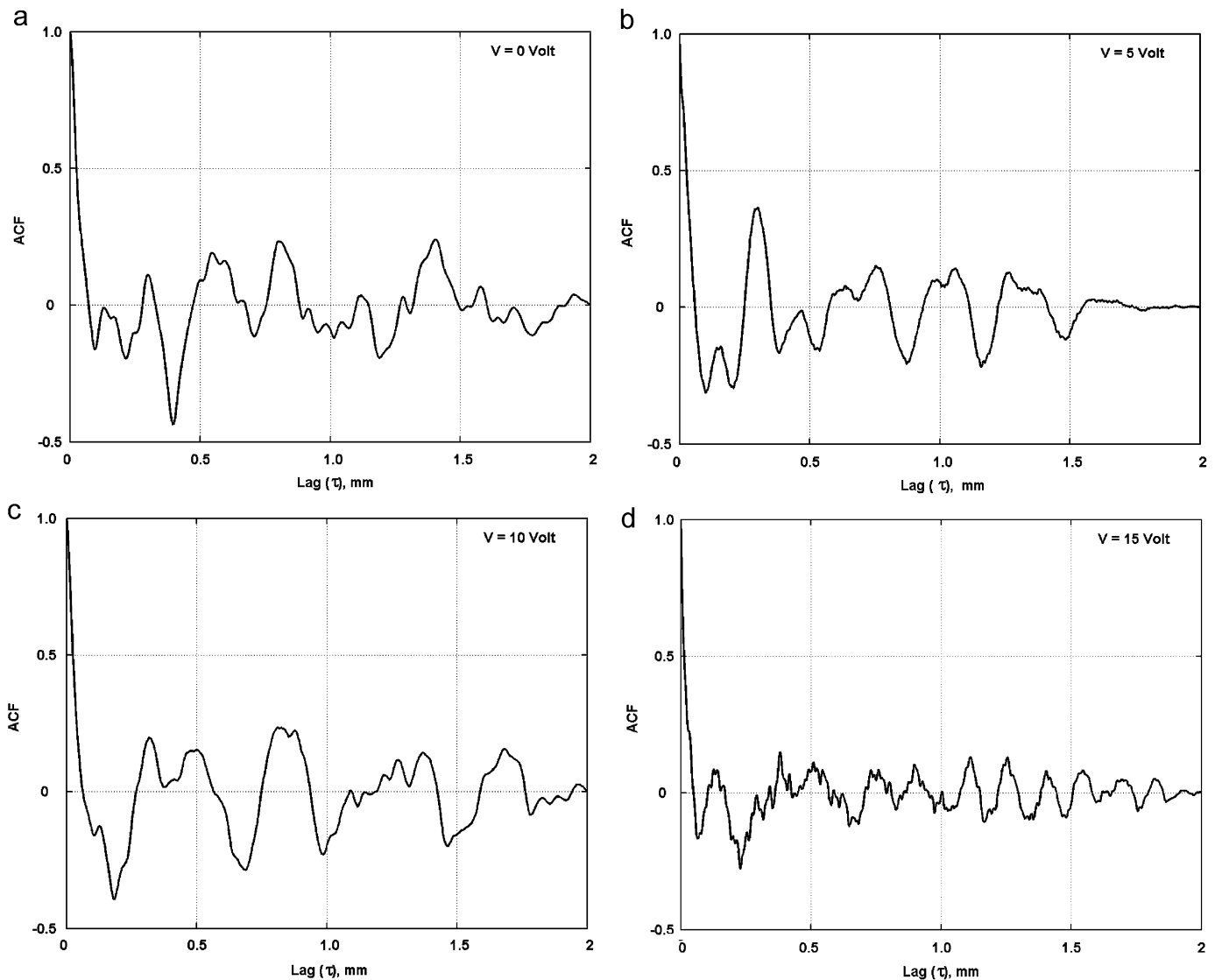


Fig. 3. (a) Plot of AutoCorrelation Function for 0 V at cutting speed 4 m/s. (b) Plot of AutoCorrelation Function for 5 V at cutting speed 4 m/s. (c) Plot of AutoCorrelation Function for 10 V at cutting speed 4 m/s. (d) Plot of AutoCorrelation Function for 15 V at cutting speed 4 m/s.

the surface is highly random [4]. Fig. 5 illustrates this idea with the help of a 2nd level ( $\lambda = 0.56$ ) ACF components at 0 and 10 V. Random component of V10 sharply drops down ( $\beta_0 = 1.52$ ) compared to that of V0 ( $\beta_0 = 6.34$ ) signifying that the surface generated under applied voltage of 10 V is less random.

#### 4. Results and discussion

To compare the relative percentage of randomness and periodicity present at different levels, a non-dimensional parameter is defined by taking the ratio of wavelength ( $\lambda$ ) and correlation length ( $\beta_0$ ) and it is termed as periodicity to randomness index. Higher value of  $\lambda/\beta_0$  suggests that correlation length is small and randomness dies out quickly at larger wavelength and surface texture becomes a harmonic one. On the other hand, lower value of  $\lambda/\beta_0$

indicates the surface to be a wide band random noise at smaller repetition distance.

The smallest frequency wave (Fig. 4(a)) strongly resembles an exponential one with a sinusoidal carrier. Moreover, the shape of the waves for different voltages is almost identical. PSDF analysis of the waves also reveals the unimodal characteristic having a wavelength of 0.85 mm. So, long range surface texture remains unaffected with increase of voltage and sinusoidal nature being more dominant; it can be taken as periodic one. It is further substantiated by the level 1 plot of  $\lambda/\beta_0$  (Fig. 6). Macro-features of electrochemically ground surface of the chosen cemented carbide, therefore, behaves less randomly and independent of voltage variation.

In the next frequency level (Fig. 4(b)), when the average wavelength is 0.55 mm the wave for all the voltages sharply dies down after a single oscillation, whereas for mechanical

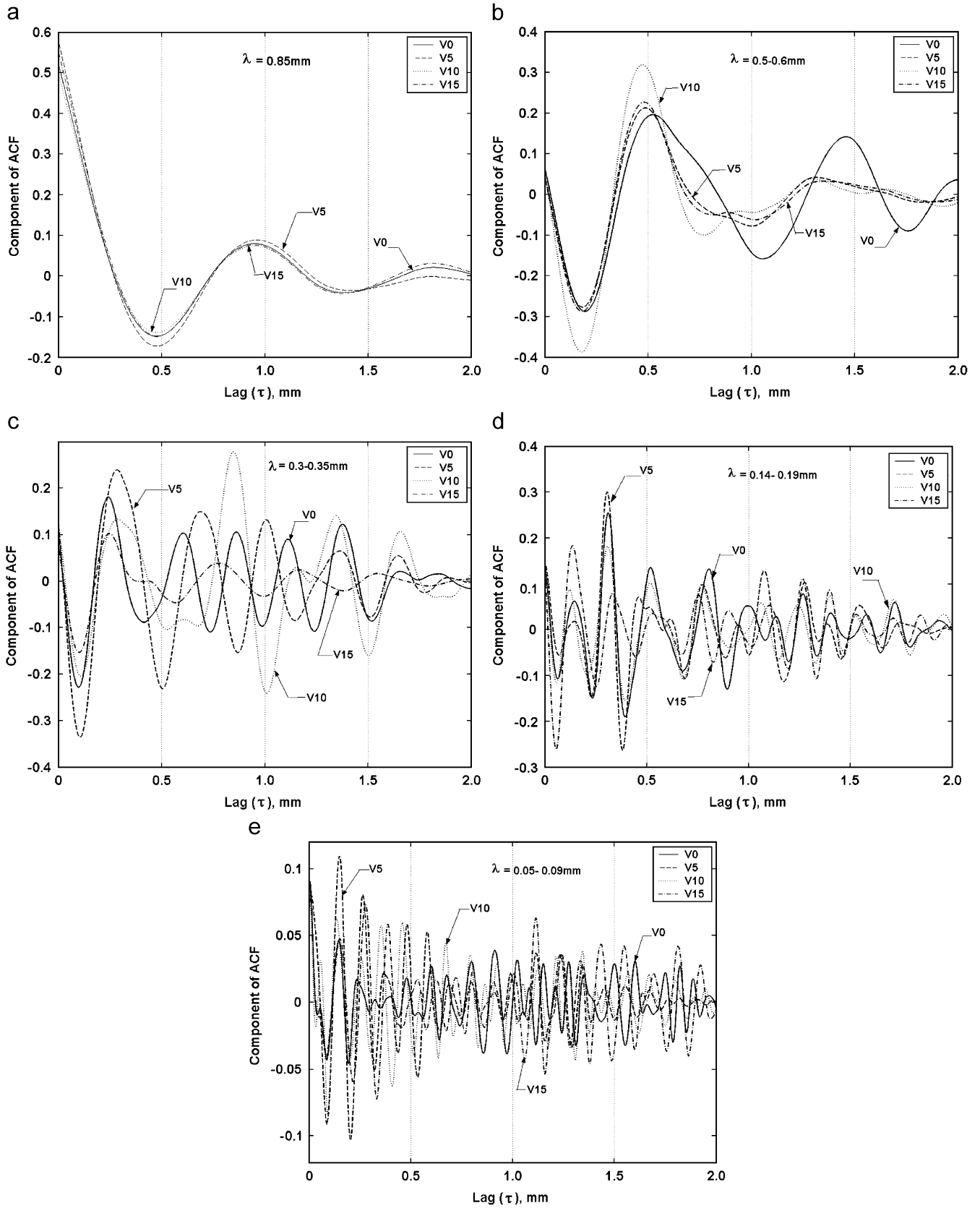


Fig. 4. (a) Components of ACF at wavelength level 1 ( $\lambda = 0.85$  mm). (b) Components of ACF at wavelength level 2 ( $\lambda = 0.5-0.6$  mm). (c) Components of ACF at wavelength level 3 ( $\lambda = 0.3-0.35$  mm). (d) Components of ACF at wavelength level 4 ( $\lambda = 0.14-0.19$  mm). (e) Components of ACF at wavelength level 5 ( $\lambda = 0.05-0.09$  mm).

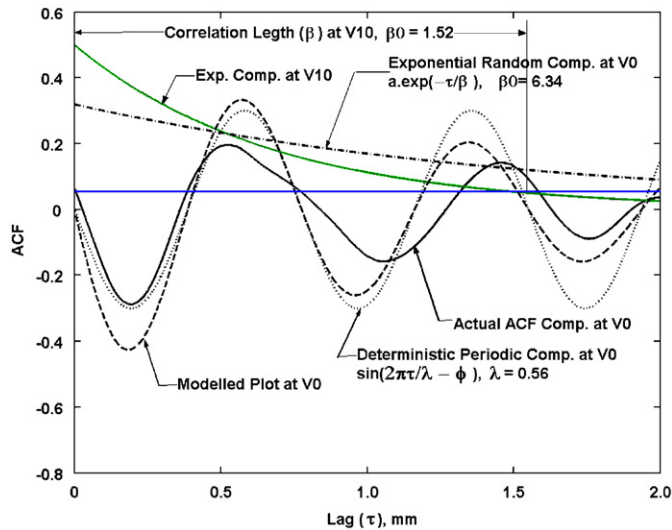


Fig. 5. Decomposition of exponential and sinusoidal components.

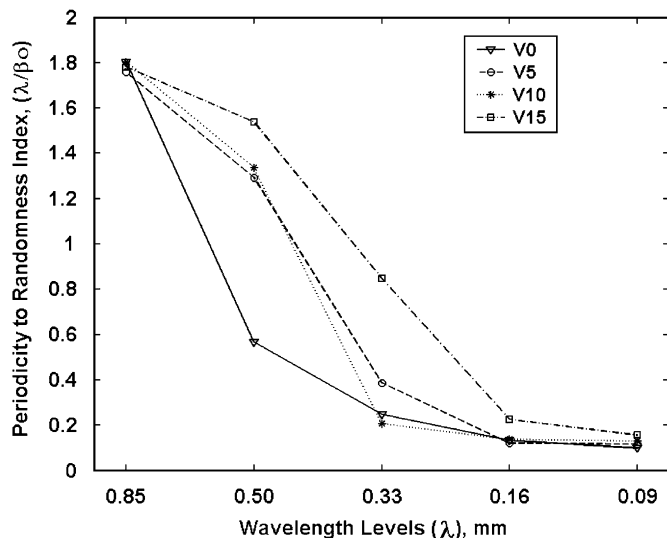


Fig. 6. Plot of  $\lambda/\beta_0$  vs. decomposition wavelength at different voltages.

grinding (when  $V = 0$  V) it continues with linearly decreasing amplitude. Lower rate of decay in amplitude means exponential nature continues over a larger distance, i.e. higher correlation length and more random event in mechanical grinding (also refer Fig. 6).

Subsequent higher order frequency plots clearly exhibit the different nature at different voltages. In Fig. 4(c) mechanical grinding continues its harmonic characteristic with almost constant amplitude suggesting more presence of random character. Wave corresponding to 5 and 10 V amplitude of oscillation decays at a slower rate, whereas for 15 V it falls sharply to very small amplitude signifying a relatively weak random feature. At higher frequency level random nature of the curves becomes more prominent as correlation length increases. In fact, 4th level ( $\lambda = 0.14$ – $0.19$  mm) and 5th level ( $\lambda = 0.05$ – $0.09$  mm) (Fig. 4(d) and (e)) components for any voltage exhibit a high degree

of randomness as the ratio  $\lambda/\beta_0$  decreases to very low value (Fig. 6).

Random shape and orientation of the abrasive grains are main source of randomness in case of purely mechanical grinding process. But when it takes place in conjunction with electrochemical action, selective and differential dissolution phenomena come into play by imparting additional randomness. In cemented carbide of P-20 grade, carbide phases with higher dissolution potential are randomly dispersed in a cobalt matrix of lower dissolution potential. Under electrolytic action, cobalt matrix is etched out at faster rate giving rise to micro-scale unevenness [11].

In this context, it is to be mentioned that while material is removed in mechanical grinding mainly by mechanical abrasion it is removed in ECG of cemented carbides by electrolytic dissolution of anodic material, chunk removal of the skeleton carbides weakened and left after selective dissolution of the soft binder cobalt and mechanical abrasion. Approximately 90% of the material is removed by electrochemical action and 10% by mechanical grinding [7]. Further the typical mean size of the grains of Co, TiC and TaC/NbC used in sintering the carbide is  $2.6 \mu\text{m}$  and that of WC is  $4.0 \mu\text{m}$  [8].

The observations of Fig. 6. can be well explained with the above considerations. When compared to ECG (V5, V10, V15), randomness in case of simple grinding (V0), increases largely at the second level for which wavelength (0.5–0.6 mm) is closer to that of grinding wheel grit size (0.45 mm). Distribution and orientation of the abrasive grains on the grinding wheel surface attributes to this effect. Medium scale randomness, therefore, is imparted mostly due to the mechanical abrasion in ECG.

With subsequent reduction in wavelength, randomness induced due to differential electrochemical dissolution of different ingredients of the chosen cemented carbide, increases at faster rate than that of pure mechanical grinding and still continues its drooping nature with further reduction of wavelength. But for mechanical grinding no significant change is observed (refer wavelength level 0.33, 0.16 and 0.09 mm in Fig. 6). The observations indicate that micro-surface roughness of cemented carbide is mostly induced by differential electrochemical reaction rates of its ingredients. Please note that the contribution of electrochemical action in material removal by ECG process is about 90%

An increase in electrode potential renders the erosion of carbide phases to take place at a faster rate under a steep voltage gradient. Small-scale surface unevenness of the chosen cemented carbide reduces as a result. It is evident from higher values of  $\lambda/\beta_0$  for V15 at all wavelength levels in Fig. 6.

## 5. Summary

ACF can be taken as an effective tool in comparative study of different superposing factors influencing the surface texture of a machined surface. Macro features of

electrochemically ground surface of the chosen cemented carbide of grade P-20 behaves less randomly and independent of voltage. Medium scale randomness is mostly imparted due to mechanical abrasion while electrochemical action contributes to micro-roughness of random nature. Increase in electrode potential reduces randomness for all frequency level. Further analysis and modeling with the aid of scale independent parameters can be extended from this platform.

## References

- [1] Venkateh K, Bobji MS, Gargi R, Biswas SK. Genesis of workpiece roughness generated in surface grinding and polishing of metals. *Wear* 1999;215–226:225–9.
- [2] Venkateh K, Bobji MS, Biswas SK. Power spectra of roughness caused by grinding of metals. *J Mater Res* 1998;319–322:225–9.
- [3] Zhou X, Xi F. Modeling and predicting surface roughness of the grinding process. *Mach Tool Manuf* 2001;42:969–77.
- [4] Bhusan B. Principles and applications of tribology. New York: Wiley; 1999.
- [5] Noble CF. Electromechanical action in peripheral electrochemical grinding. *Ann CIRP* 1983;32/1:123–7.
- [6] Nandiv S, Lenze E, Geva M. Peripheral electrochemical grinding of cintered carbides-effect on surface finish. *Wear* 1976;38:325–39.
- [7] Benedict GF. Nontraditional manufacturing processes. New York and Basel: Marcel Dekker Inc.; 1987.
- [8] Trent EM, Wright PK. Metal cutting. New Delhi, India: Reed Elsevier India Private Limited; 2006.
- [9] Bendat JS, Piersol AG. Engineering application of correlation and spectral analysis. New York: Wiley; 1986.
- [10] Bhattacharyya A. Metal cutting theory and practice. Calcutta: New Central Book Agency; 1984.
- [11] Puri A. Analysis of electrochemical grinding process through response surface and Scanning Electron Microscope study. M.E. Thesis, Jadavpur University; 2003.